MicroRNA-744-5p inhibits glioblastoma malignancy by suppressing replication factor C subunit 2

FEI FAN[1*], DONGXIAO YAO[1*], PENGFEI YAN[1], XIAOBING JIANG[1] and JIE HU[2]

[1]Department of Neurosurgery, Union Hospital, Tongji Medical College, Huazhong University of Science and Technology, Wuhan, Hubei 430022; [2]Department of Neurosurgery, General Hospital of The Yangtze River Shipping, Jiangan, Wuhan, Hubei 430010, P.R. China

Received December 10, 2020; Accepted April 13, 2021

DOI: 10.3892/ol.2021.12869

Abstract. Glioblastoma (GBM) is the most common malignant primary brain tumor, accounting for ~57% of all gliomas and 48% of all malignant primary central nervous system tumors in the United States. Abnormal expression of the replication factor C subunit 2 (RFC2) gene and microRNA (miR)-744-5p is associated with tumorigenic characteristics, including cellular proliferation, migration and invasiveness. However, the mechanism underlying the interaction between miR-744-5p and RFC2 in GBM remains unknown. Reverse transcription-quantitative (RT-q) PCR analysis of RFC2 and miR-744-5p was performed using GBM tumor tissues and cells, and the association between miR-744-5p and RFC2 was determined by dual-luciferase reporter assay. Cell Counting Kit 8, 5-bromo-2-deoxyuridine (BrdU), wound-healing and cellular adhesion assays, as well as the detection of caspase-3 activity and western blotting were used to detect cellular proliferation, migration and adhesion, caspase-3 activity, and Bax and Bcl-2 protein expression, respectively, in GBM cells. The results of the present study demonstrated that RFC2 expression was increased in GBM tissues and cell lines. Overexpression of RFC2 promoted cellular proliferation, migration, adhesion and an increase in Bcl-2 protein levels, and suppressed cellular caspase-3 activity and Bax protein expression, while silencing RFC2 resulted in the opposite effect. The effects of miR-744-5p inhibition were similar to those of RFC2 overexpression. Moreover, miR-744-5p was found to target RFC2 in GBM cells, and inhibiting the expression of RFC2 suppressed GBM tumorigenesis. In conclusion, the present study demonstrated that miR-744-5p targets RFC2 and suppresses the progression of GBM by repressing cellular proliferation, migration and Bcl-2 protein expression, and effectively promoting caspase-3 activity and Bax protein expression. These findings suggest a new target for the clinical treatment and improved prognosis of patients with GBM in the future.

Correspondence to: Dr Xiaobing Jiang, Department of Neurosurgery, Union Hospital, Tongji Medical College, Huazhong University of Science and Technology, 1277 Liberation Avenue, Wuhan, Hubei 430022, P.R. China
E-mail: jxb917@126.com

Dr Jie Hu, Department of Neurosurgery, General Hospital of The Yangtze River Shipping, 5 Huiji Road, Jiangan, Wuhan, Hubei 430010, P.R. China
E-mail: jiehu2558@163.com

*Contributed equally

Key words: microRNA-744-5p, replication factor C subunit 2, glioblastoma, proliferation, migration, apoptosis

Introduction

Glioblastoma (GBM) is a common malignant primary brain tumor that accounts for ~57% of all gliomas and 48% of all malignant primary tumors of the central nervous system in the United States (1). The prevalence of GBM is highest in North America and Australia, as well as Northern and Western Europe (2). Caucasian patients have the poorest survival rates and highest incidence of GBM (3), and treatment strategies such as surgery, radiotherapy and chemotherapy appear to be ineffective. Moreover, poor prognosis and low long-term survival remain challenging issues (4), though precision oncology and targeted gene therapy herald much promise in developing more efficacious treatments for patients with GBM.

MicroRNAs (miRNAs/miRs) are abundant small non-coding RNAs, ~20-24 nucleotides in length, that regulate gene expression by inhibiting translation or degrading messenger RNA (5,6). A cluster of miRNAs has been shown to affect tumor cellular biological processes and to serve as potential diagnostic targets in various human cancers (7,8). For example, miR-744-5p has been associated with numerous cancers and plays an important role in tumor progression characteristics, including cellular proliferation, invasiveness and apoptosis (9-11). Accumulating evidence suggests that miR-744-5p may also be a promising therapeutic target for cancer treatment (12,13), and has also been reported to suppress cellular proliferation and invasiveness in ovarian (14) and lung cancer (15). Further studies have shown that miR-744-5p is abnormally expressed in GBM, regulating its occurrence and development (16,17). Nevertheless, the underlying mechanisms by which miR-744-5p acts on GBM require further investigation.

The replication factor C subunit 2 (RFC2) gene is located on chromosome 7q11.23 and consists of 11 exons, encoding a member of the activator 1 small subunit family. RFC2 plays an important role in the elongation of primed DNA templates by DNA polymerase δ and ε (18). Upregulated RFC2 expression has been associated with a number of cancers, such as nasopharyngeal (19) and esophageal squamous cell carcinoma (20). However, to the best of our knowledge, only a single study has reported the involvement of RFC2 in GBM, in which RFC2 was indicated to enhance temozolomide (TMZ) cytotoxicity (21). Notably, RFC2 was found to be a direct target of miR-744-5p in the progression of colorectal cancer cell tumorigenicity (22). However, little is known about the expression pattern and biological functions of RFC2 in GBM, including its interaction with miR-744-5p. Therefore, it may be beneficial to elucidate the biological role of RFC2 and its potential interaction with miR-744-5p therein.

Thus, the aim of the present study was to explore a novel interactome, miR-744-5p-RFC2, and to determine the effects of miR-744-5p and RFC2 in GBM. We hypothesized that miR-744-5p suppressed GBM by inhibiting RFC2, which may provide novel targets for the clinical treatment of GBM, and improve future patient prognosis.

Materials and methods

Bioinformatics analysis. Gene Expression Profiling Interactive Analysis (GEPIA; http://gepia2.cancer-pku.cn/#index), including gene expression profiling data from The Cancer Genome Atlas project, was performed to screen differentially expressed genes (DEGs, criteria: $|\log_2 FC| \geq 2$ and $P<0.01$) and survival-related genes (criteria: $P<0.01$) associated with GBM. Then, the DEGs and survival-associated genes were overlapped using Venny 2.1.0 (https://bioinfogp.cnb.csic.es/tools/venny/), and STRING (https://string-db.org/) was used to predict the protein-protein interactions between the overlapping genes. Finally, the ENCORI starBase (http://starbase.sysu.edu.cn/index.php), TargetScan Human 7.2 (http://www.targetscan.org/vert_71/) and miRDB.org algorithms (http://mirdb.org/) were used to predict the upstream miRNAs of key genes.

Tissue samples. GBM tissues (n=39) and normal adjacent tissues (n=39) were collected from Union Hospital, Tongji Medical College, Huazhong University of Science and Technology (Wuhan, China) between April 2015 and October 2019. Inclusion criteria included: i) Postoperative pathology diagnosed as GBM; and ii) Complete patient information obtained. Exclusion criteria included: i) Patients who underwent radiotherapy and chemotherapy before surgery; ii) Patients with a history of another kind of malignant cancer; and iii) Patients with serious heart, liver, spleen, lung or kidney diseases. The study protocol was approved by the Ethics Committee of Union Hospital on September 12, 2018 [approval. no. (2018)(216)], and all patients provided written informed consent. The clinical characteristics of the GBM subjects are presented in Table I. The patient aged 45-70 years old, with a mean age of 52.6±9.3 years.

Cell culture and transfection. The human GBM cell lines, U87 (cat. no. HTB-14; GBM of unknown origin) and A172 (cat. no. CRL-1620) were purchased from the American Type Culture Collection. U251 (cat. no. TCHu 58) and SHG44 (cat. no. TCHu 48) cells were purchased from the cell bank of the Chinese Academy of Sciences (Shanghai, China). Normal human astrocyte (NHA) cells (cat. no. 1800) were purchased from ScienCell Research Laboratories, Inc. U251, SHG44, A172 and NHA cells were maintained in DMEM and U87 cells were maintained in MEM, both with 10% fetal bovine serum (FBS) (Invitrogen; Thermo Fisher Scientific, Inc.), at 37˚C (5% CO_2 and 90% humidity). All cell lines were verified by short tandem repeat authentication.

For transfection, the RFC2-overexpression (RFC2-OE) vector, pcDNA 3.1 empty vector [used as the RFC2-OE negative control (NC)], si-NC, si-RFC2, miR-744-5p inhibitor, miR-744-5p mimics, mimic-NC and inhibitor-NC were all purchased from Shanghai Tuoran Co., Ltd. A total of $3x10^5$/well U251 and U87 cells were cultured in 24-well plates and transfected with either si-NC, si-RFC2, RFC2-OE, miR-744-5p inhibitor, miR-744-5p mimic or pcDNA 3.1, mimic-NC or inhibitor-NC, at a concentration of 50 nM using Lipofectamine® 3000 (Invitrogen; Thermo Fisher Scientific, Inc.), and maintained at 37˚C for 48 h before subsequent experiments were performed. The sequences of RFC2-OE, si-RFC2, miR-744-5p inhibitor, the miR-744-5p mimics and their corresponding NC are presented in Table SI.

RNA extraction and reverse transcription-quantitative (RT-q) PCR. Total RNA from the tissue specimens and cell lines was isolated using TRIzol® reagent following the manufacturer's instructions (Thermo Fisher Scientific, Inc.). Subsequently, total RNA was reverse transcribed into cDNA using the PrimeScript First Strand cDNA Synthesis kit (Takara Biotechnology Co., Ltd.). The targeted reverse transcription of miRNA was performed using the Hairpin-it miRNA qPCR Quantitation Kit (Shanghai GenePharma Co., Ltd.). Then, SYBR Premix Ex Taq (Takara Biotechnology Co., Ltd.) was used for qPCR, performed on an ABI Prism 7900 Detector System (Thermo Fisher Scientific, Inc.). The qPCR conditions were 1 cycle at 95˚C for 20 sec, followed by 40 cycles of 1 min each at 95˚C, and 20 sec at 60˚C. Relative expression levels were normalized to that of U6 and β-actin, corresponding to miRNA and mRNA, respectively. The expression levels were calculated using the $2^{-\Delta\Delta Cq}$ method (23). The primer sequences are listed in Table II.

Western blotting. Total proteins from the U251 and U87 cells were extracted using radioimmunoprecipitation assay lysis buffer (MilliporeSigma), and the total protein content was quantified using a BCA detection kit (Thermo Fisher Scientific, Inc.). Then, the proteins (30 μg per well) were separated by 10% SDS-PAGE and subsequently transferred onto PVDF membranes (EMD Millipore). The membranes were blocked with 5% skim milk for 1 h at 25˚C, and then incubated with the following primary antibodies at 4˚C for 12 h: Anti-RFC2 (cat. no. ab174271; 1:10,000; Abcam), goat anti-rabbit Bax (cat. no. ab32503; 1:2,000; Abcam), goat anti-rabbit Bcl-2 (cat. no. ab182858; 1:2,000; Abcam) and anti-β-actin (cat. no. ab8226; 1:10,000; Abcam). After washing three times with TBS containing 0.05% Tween 20 (TBST), the membranes were incubated then with the following secondary antibodies:

Table I. Association of RFC2 or miR-744-5p expression with the epidemiologic features of 39 patients with glioblastoma.

	Expression of RFC2			Expression of miR-744-5p		
Clinical features (n)	Low	High	P-Value	Low	High	P-value
Age						
<60 (23)	10	13	0.4325	11	12	0.7491
≥60 (16)	9	7		7	9	
Sex						
Male (20)	9	11	0.6337	10	10	0.6211
Female (19)	10	9		8	11	
Grade						
+II (15)	12	3	0.0020	3	12	0.0096
III+IV (24)	7	17		15	9	
Tumor size, cm						
<5 (18)	13	6	0.0164	7	12	0.0154
≥5 (21)	6	14		14	6	
IDH status						
Wild-type (20)	12	8		7	13	0.3373
Mutated (19)	7	12		11	8	
Distant metastasis						
Metastasis (21)	5	16	0.0008	15	6	0.0006
No metastasis (18)	14	4		3	15	
	RFC2 expression			miR-744-5p expression		
Clinical feature (n)	Low	High	P-Value	Low	High	P-value
Age, years						
<60 (23)	10	13	0.4325	11	12	0.7491
≥60 (16)	9	7		7	9	
Sex						
Male (20)	9	11	0.6337	10	10	0.6211
Female (19)	10	9		8	11	
Grade						
+II (15)	12	3	0.0020	3	12	0.0096
III+IV (24)	7	17		15	9	
Tumor size, cm						
<5 (18)	13	6	0.0164	7	12	0.0154
≥5 (21)	6	14		14	6	
IDH status						
Wild-type (20)	12	8	0.1481	7	13	0.3373
Mutated (19)	7	12		11	8	
Distant metastasis						
Metastasis (21)	5	16	0.0008	15	6	0.0006
No metastasis (18)	14	4		3	15	

RFC2, replication factor C subunit 2; miR, microRNA; IDH, isocitrate dehydrogenase.

Goat anti-rabbit for RFC2 (cat. no. ab205718; 1:2,000; Abcam) and goat anti-mouse for β-actin (cat. no. ab175783; 1:2,000; Abcam) for 1 h at 25˚C. Finally, positive bands were visualized with the Immobilon™ Western Chemiluminescent horseradish peroxidase (HRP) substrate (EMD MilliporeSigma). The densities of the bands was determined using ImageJ software version 1.53 (National Institutes of Health).

Cell Counting Kit 8 (CCK-8) assay. The CCK-8 (Sangon Biotech Co., Ltd.) was used to determine the viability of U251 and

Table II. Primer sequences.

Primer	Sequence
RFC2	
Forward	5'-CCTGAGGTCCTTCTGGTGGT-3'
Reverse	5'-CAACGTCAATGCCCCTGTCA-3'
miR-744-5p	
Forward	5'-TGCGGGGCTAGGGCTA-3'
Reverse	5'-CGGCCCAGTGTTCAGACTAC-3'
miR-2355-5p	
Forward	5'-ATTGTCCTTGCTGTTTGGAGAT-3'
Reverse	5'-GCGAGCACAGAATTAATACGAC-3'
miR-122-5p	
Forward	5'-TATTCGCACTGGATACGACACAAC-3'
Reverse	5'-GCCCGTGGAGTGTGACAATGGT-3'
GAPDH	
Forward	5'-CCAGGTGGTCTCCTCTGA-3'
Reverse	5'-GCTGTAGCCAAATCGTTGT-3'
U6	
Forward	5'-CTCGCTTCGGCAGCACA-3'
Reverse	5'-AACGCTTCACGAATTTGCGT-3'

RFC2, replication factor C subunit 2; miR, microRNA.

U87 cells. Transfected cells ($2x10^3$/well) in 96-well plates were incubated for 0, 24, 48 and 72 h. Then, 10 μl CCK-8 reagent was added to each well and the cells were incubated for a further 2 h. The absorbance was measured at an optical density of 450 nm using a multimode microplate reader (Tecan Group, Ltd.).

5-bromo-2-deoxyuridine (BrdU) assay. Cellular proliferation was evaluated using the BrdU Cell Proliferation Assay Kit (Cell Signaling Technology, Inc.) per the manufacturer's instructions. U251 and U87 cells were seeded into 96-well plates ($2x10^4$ cells per well) and cultured in FBS-free medium for 24 h to synchronize the cell cycle. Then, the medium was removed and the cells were labeled with 1X BrdU solution (prepared in cell culture medium) for 6 h at 37˚C to induce proliferation. The labeling medium was removed, and the cells were fixed and denatured using the supplied fixation/denaturation solution. BrdU mouse mAb was then added and the cells were incubated for 2 h at 37˚C. Anti-mouse immunoglobulin G and HRP-linked antibody were used to detect the binding antibody, and HRP substrate (3,3,5,5-tetramethylbenzidine) was added for color development. Finally, the absorbance at 450 nm was determined using a multimode microplate reader (Tecan Group, Ltd.).

Wound-healing assay. The migratory ability of U251 and U87 cells was evaluated by wound-healing assay. Cells were seeded into 6-well plates ($2x10^5$/well), cultured to 80% density and subsequently, 200-μl pipette tips were used to create wounds in the center of each well. After incubation with FBS-free medium for 24 h at 37˚C, the wound was photographed using an optical microscope (Olympus Corporation) at x100 magnification. The wound closure was measured using the following formula: (W0 h-W24 h)/W0 h x100%, where W is the width.

Cellular adhesion Assay. A 96-well plate was coated with collagen I solution (40 μg/ml; Sigma-Aldrich; Merck KGaA) and stored at 4˚C for 12 h. U251 and U87 cells ($2x10^5$ cells/ml) were cultured in FBS-free DMEM for 8 h before harvesting by trypsinization. Then, the cells were collected and suspended in 100 μl DMEM with 0.1% BSA in the coated 96-well plate, and incubated at 37˚C for 20 min. Subsequently, the cells were incubated with medium containing 10% FBS for 4 h at 37˚C. Then, 10 μl MTT substrate (MilliporeSigma) was added to each well and the plate was incubated for a further 2 h at 30˚C. The cells were then washed twice with PBS and 100 μl DMSO was added to each well. Absorbance was measured at a wavelength of 570 nm using a multimode microplate reader (Tecan Group, Ltd.).

Caspase activity assay. U251 and U87 cells were seeded into 96-well plates ($3x10^5$ cells per well). Caspase-3 assay loading solution (Cell Signaling Technology, Inc.) was prepared by adding the caspase-3 substrate to DL-dithiothreitol reagent according to the manufacturer's instructions. Cells were collected at 80% density and lysed with ice-cold cell lysis buffer for 10 min. Subsequently, loading solution (100 μl/well) was added to each sample and incubated at 37˚C for 2 h. The absorbance was then measured at a wavelength of 405 nm using a multimode microplate reader (Tecan Group, Ltd.).

Dual-luciferase reporter assay. The psiCHECK2-RFC2-3' untranslated region (3'-UTR) wild-type vectors and psiCHECK2 RFC2-3'-UTR mutated vectors were purchased from Weizhen Bio (Shanghai, China). U251 and U87 cells were co-transfected with the vectors and negative control (NC) or miR-744-5p mimics using Lipofectamine® 3000, and cultured in a 24-well plate. After 48 h, the dual-luciferase reporter assay System (Promega Corporation) was used to detect the firefly and *Renilla* luciferase activities. Relative luciferase activity was normalized to the activity of *Renilla* luciferase (internal control).

RNA pull-down analysis. The biotin-labeled miR-2355-5p (Bio-miR-2355-5p, 5'-AUCCCCAGAUACAAUGGACAA-biotin-3'), miR-122-5p (Bio-miR-122-5p, 5'-AACGCCAUUAUCACACUAAAUA-biotin-3') and miR-744-5p (Bio-miR-744-5p, 5'-UGCGGGGCUAGGGCUAACAGCA-biotin-3'), as well as negative controls (Bio-NC, 5'-GUGCACGAAGGCUCAUCAUU-biotin-3') were purchased from Guangzhou RiboBio Co., Ltd, and were used to transfect both U251 and U87 cells for 48 h at 37˚C using Lipofectamine® 3000. Next, the cells were collected and lysed using 0.5 ml lysis buffer, containing 25 mM Tris-HCl (pH 7.5), 70 mM KCl, 2.5 mM EDTA, 0.05% NP-40, protease inhibitor cocktail (Sigma-Aldrich; Merck KGaA) and RNase inhibitors (Thermo Fisher Scientific, Inc.), for 20 min on ice. The mixture was centrifuged at 1,400 x g at 4˚C for 20 min, and 0.5 ml supernatant lysate was collected. The streptavidin beads (50 μl; cat. no. 88816; Thermo Fisher Scientific, Inc.) were washed and added to the supernatant lysates, and then incubated at 4˚C on a rotating platform for 12 h. The following day, the beads were washed twice with cold lysis buffer, three times with low salt buffer solution, and once with high salt buffer solution;

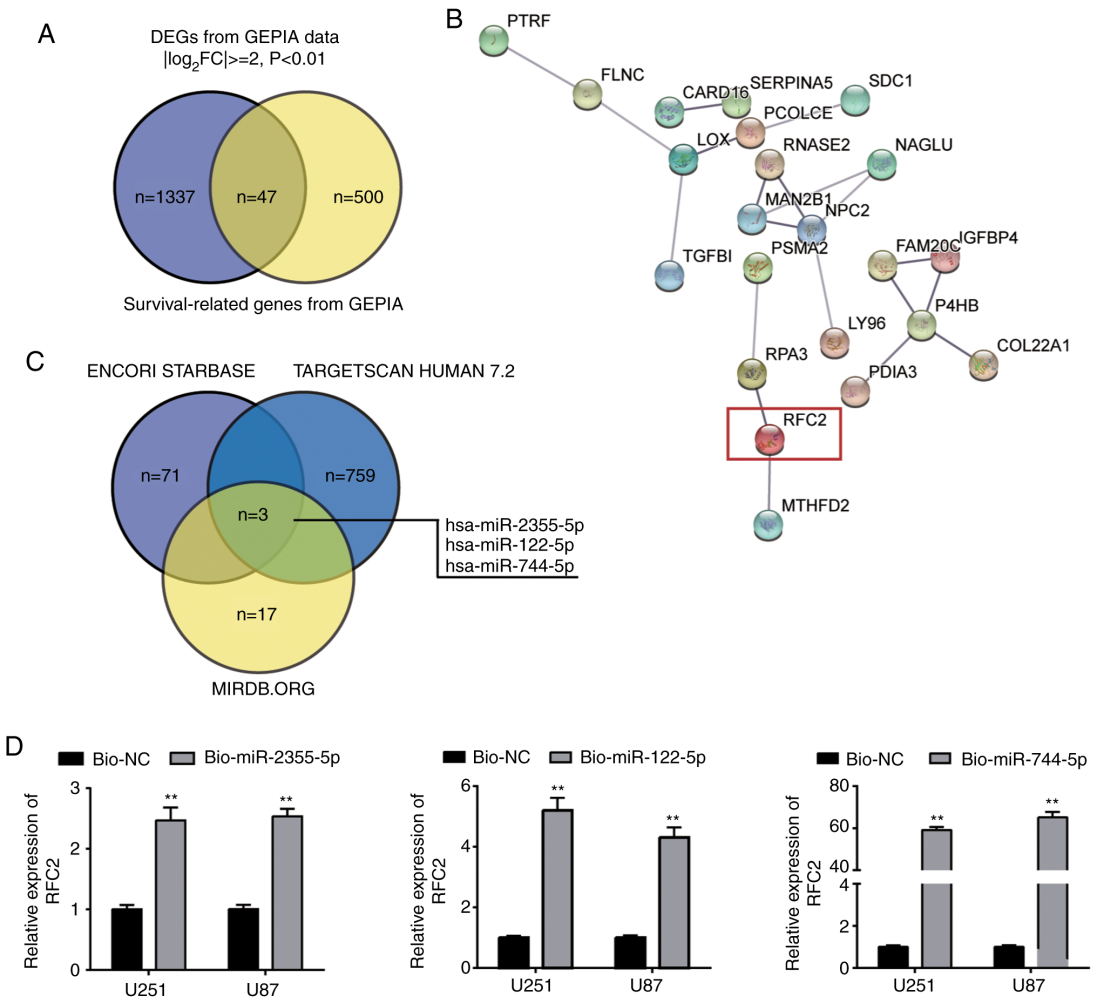

Figure 1. Identification of study objects of interest. (A) Venn diagram demonstrating the intersection of DEGs and survival-related genes in GBM from GEPIA database. (B) STRING results demonstrating the interaction network of the 47 intersected genes from (A). (C) Intersection of upstream miRNAs of RFC2 from the ENCORI starBase, TargetScan Human 7.2 and miRDB.org algorithms; log_2FC: log_2fold change. (D) RFC2 was mainly pulled down in the GBM cells transfected with bio-miR-744-5p. Bio-NC, Biotin-labelled NC; Bio-miR-2355-5p, Biotin-labeled miR-2355-5p; Bio-miR-122-5p, Biotin-labeled miR-122-5p; Bio-miR-744-5p, Biotin-labeled miR-744-5p. **P<0.001, compared with Bio-NC using one-way ANOVA with Tukey's test. DEG, differentially expressed gene; GBM, glioblastoma; GEPIA, Gene Expression Profiling Interactive Analysis; RFC2, replication factor C subunit 2; miR, microRNA; NC, negative control.

the specifically-bound RNAs were purified using the RNeasy Mini Kit (QIAGEN). Finally, the enrichment of RFC2 was detected by performing RT-qPCR.

Statistical analysis. All analyses were performed using GraphPad Prism 8.0 software (GraphPad Software, Inc.). Paired Student's t-test (two-tailed) was used to compare the differences between two groups, while the differences between three or more groups were determined by one-way ANOVA with Dunnett's (comparisons with one group) or Tukey's (comparisons with more than one group) post hoc test. The correlation between miR-744-5p and RFC2 expression levels was determined by Pearson's correlation analysis. Data are presented as the mean ± standard deviation, and P<0.05 was considered to indicate a statistically significant difference.

Results

Identification of study objects of interest. DEGs and survival-related genes for GBM were acquired from the GEPIA database, which is a gene expression profiling interactome analysis tool that includes gene expression profiling data from The Cancer Genome Atlas project. GEPIA yielded 1,384 DEGs with the criteria of $|log_2FC| \geq 2$ and P<0.01, and 547 GBM survival-related genes with the criterial of P<0.01. Among these genes, 47 were both DEGs and GBM survival-related (Fig. 1A). By performing STRING analysis of the 47 genes, 22 were found to be closely related (Fig. 1B). The STRING network indicated that RFC2 had been studied in glioma once, and it was reported to be related to drug cytotoxicity; furthermore, the knockdown of RFC2 led to reduced cell viability (21). Nonetheless, how RFC2 affects other GBM cell phenotypes has not been extensively studied. Therefore, RFC2 was chosen as a gene of interest. The ENCORI starBase, TargetScan Human 7.2 and miRDB.org algorithms were used to predict the upstream miRNAs of RFC2, and three overlapping miRNAs (miR-2355-5p, miR-122-5p and miR-744-5p) were identified (Fig. 1C). After constructing bio-miR-2355-5p, bio-miR-122-5p and bio-744-5p, these plasmids showed high transfection efficiency in U251 and U87 (Fig. S1). After RNA pull-down analysis, it was observed that the association between RFC2 and miR-744-5p was stronger than that with miR-2355-5p or miR-122-5p (Fig. 1D). Therefore,

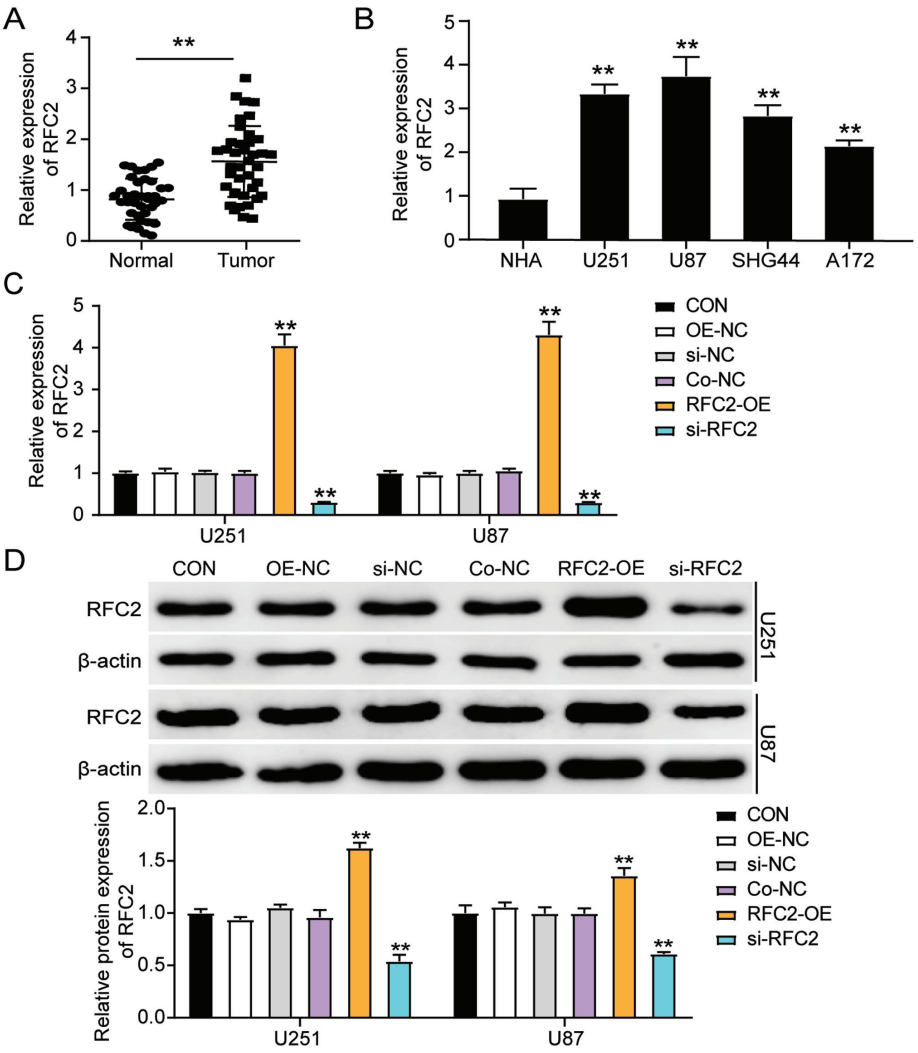

Figure 2. RFC2 expression is upregulated in GBM tissues and cells. (A) RT-qPCR analysis of gene expression of RFC2 in GBM tumor tissues (n=39) and adjacent controls (n=39) from patients with GBM. **P<0.001, compared with Normal group using paired Student's t-test. (B) RT-qPCR analysis of the RFC2 expression in GBM cell lines (U251, U87, SHG44 and A172) and the normal astrocyte NHA cell line. **P<0.001, compared with NHA using one-way ANOVA with Dunnett's test. (C) RT-qPCR analysis of gene expression of RFC2 in U251 and U87 cells transfected with NC, RFC2-OE and si-RFC2. (D) Western blot analysis of RFC2 protein expression in U251 and U87 cells transfected with NC, RFC2-OE and si-RFC2. (C and D) **P<0.001, compared with CON using one-way ANOVA with Dunnett's test. CON, blank control; si-NC, si-RFC2 negative control; OE-NC, pcDNA 3.1 empty vector; Co-NC, si-NC+OE-NC; si-RFC2, siRNA-RFC2; RFC2-OE, RFC2-overexpression; RFC2, replication factor C subunit 2; GBM, glioblastoma; RT-q, reverse transcription-quantitative; si(RNA), small interfering; OE, overexpression; NC, negative control.

the involvement of RFC2 mRNA and miR-744-5p miRNA in GBM was investigated further.

RFC2 expression is upregulated in GBM tissues and cell lines. To elucidate whether RFC2 is involved in GBM, RFC2 expression was first detected in tumor tissues and corresponding normal tissues from patients with GBM. The results showed that RFC2 expression increased 1.5-fold compared to normal control tissues (Fig. 2A). RFC2 gene expression was also detected in NHAs and GBM cells (U251, U87, SHG44 and A172), and was significantly increased in the GBM cell lines compared to NHA cells. In particular, U251 and U87 cells showed more than a 3-fold increase in RFC2 expression compared with NHA cells. Therefore, U251 and U87 cells were chosen for subsequent experiments due to having the highest expression of RFC2 (Fig. 2B). To further explore the effects of RFC2 in GBM, U251 and U87 cells were transfected with si-NC, OE-NC (pcDNA 3.1 empty vector), Co-NC (si-NC+OE-NC), RFC2-overexpression (OE),or si-RFC2 constructs. Cells transfected with RFC2-OE displayed ~4-fold upregulated RFC2 levels compared with the control cells, while cells transfected with si-RFC2 exhibited an ~70% decrease in RFC2 levels compared with the control cells (Fig. 2C). Furthermore, the protein expression levels of RFC2 increased more than 1.4-fold in cells transfected with RFC2-OE, with an ~60% decrease in protein levels observed in si-RFC2 cells compared with the control cells (Fig. 2D). As the Co-NC exerted no obvious effect on RFC2 expression, Co-NC was used as the NC group in subsequent experiments.

RFC2 promotes cellular proliferation, migration and adhesion, and suppresses apoptosis in GBM. To determine whether RFC2 promotes GBM tumorigenesis, a CCK-8 assay was performed using transfected U251 and U87 cells. Cells transfected with RFC2-OE exhibited higher proliferative capacity, while cells transfected with si-RFC2 proliferated to a lower degree than the control cells (Fig. 3A). Moreover,

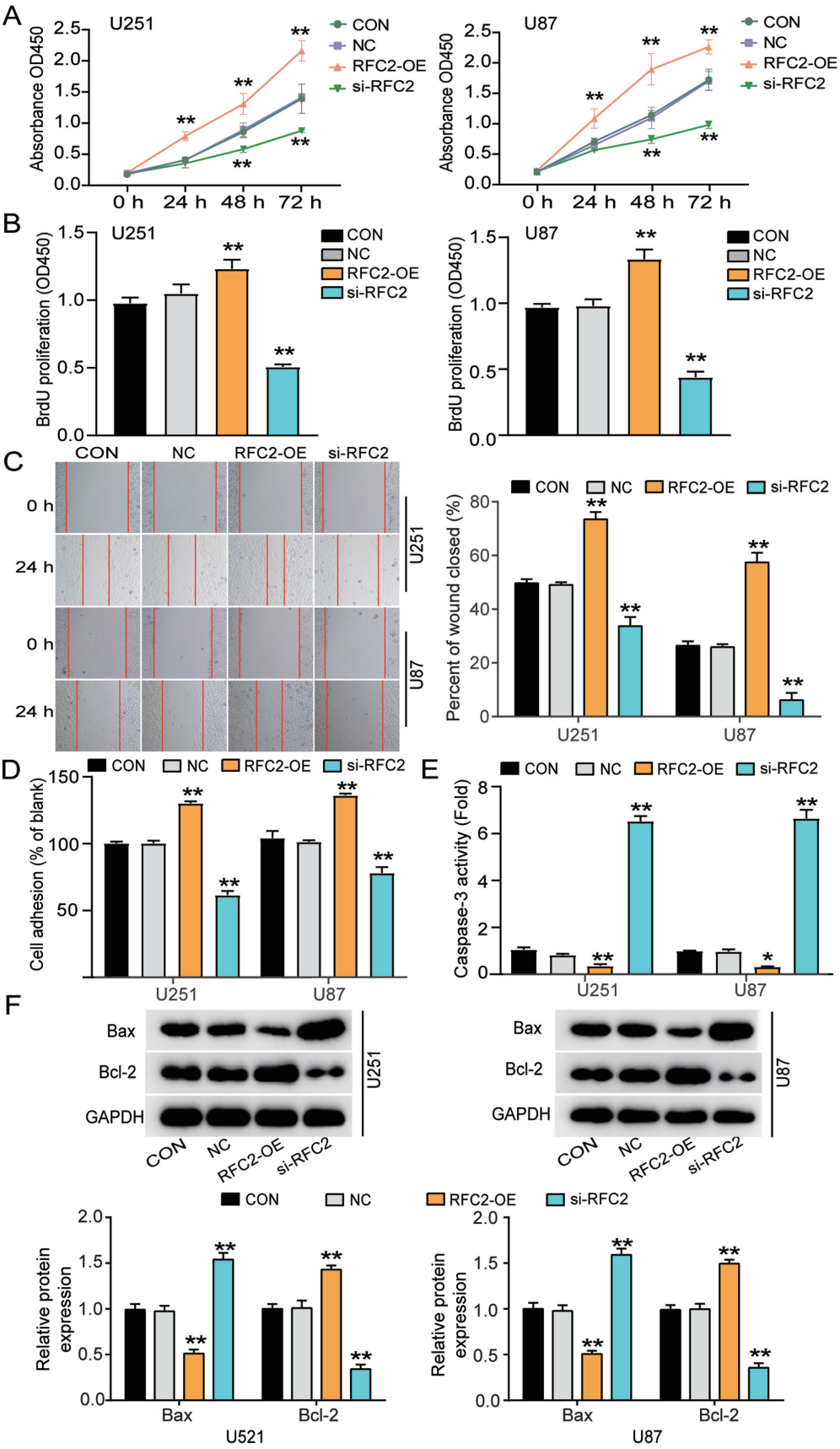

Figure 3. RFC2 promotes cellular proliferation, migration and adhesion, and suppresses cell apoptosis in glioblastoma. (A) Viability of U251 and U87 cells transfected with NC, RFC2-OE and Si-RFC2 was determined by Cell Counting Kit 8 assay. (B) Cellular proliferation was detected in U251 and U87 cells transfected with NC, RFC2-OE and si-RFC2 by BrdU assay. (C) Wound-healing assay was performed in U251 and U87 cells transfected with NC, RFC2-OE and si-RFC2. (D) Adhesion ability was detected in U251 and U87 cells transfected with NC, RFC2-OE and si-RFC2. (E) Caspase3 activity was determined in U251 and U87 cells transfected with NC, RFC2-OE and si-RFC2 by caspase3 activity assay kit. (F) Protein expression levels of Bax and Bcl-2 were determined in U251 and U87 cells transfected with NC, RFC2-OE and si-RFC2 by western blotting. *P<0.05 and **P<0.001, compared with CON using one-way ANOVA with Dunnett's test. CON, blank control; NC, negative control; si-RFC2, siRNA-RFC2; RFC2-OE, RFC2-overexpression; RFC2, replication factor C subunit 2.

according to the results of the BrdU assay, cells transfected with RFC2-OE exhibited an ~30% enhancement in proliferation, while cells transfected with si-RFC2 indicated reduced proliferation (~50%) compared with the control cells (Fig. 3B). A wound-healing assay was performed to assess the migratory capacity of the transfected cells. The results showed a 30% increase in the migratory ability of cells transfected with RFC2-OE, and a 50% decrease in the migratory ability of cells transfected with si-RFC2 compared with the control cells (Fig. 3C). Furthermore, adhesion ability was elevated by ~30% in cells transfected with RFC2-OE, while cells transfected with si-RFC2 showed ~30% reduced cell adhesion ability compared with the control cells (Fig. 3D). Additionally, the levels of caspase-3 activity were elevated 6-fold in cells transfected with si-RFC2, while cells transfected with RFC2-OE indicated reduced levels of caspase-3 activity by 70% compared to control cells (Fig. 3E). Furthermore, western blot analysis showed that compared with the control group, Bax protein expression was decreased and Bcl-2 expression was increased in U251 and U87 cells overexpressing RFC2, while the trend was opposite in cells with low expression of RFC2 (Fig. 3F). Therefore, these results demonstrated that RFC2 promoted cell proliferation, migration, and adhesion, and suppressed cell apoptosis in GBM.

RFC2 is a target of miR-744-5p in GBM. The TargetScan Human 7.2 database was used to identify potential miRNAs targeting RFC2. The analysis identified miR-744-5p as a potential miRNA that could interact with the 3'UTR of RFC2 mRNA; the binding sequences are displayed in Fig. 4A. Subsequently, U251 and U87 cells were successfully transfected with miR-744-5p mimics and inhibitor (Fig. S2). The results showed that U251 and U87 cells co-transfected with wild-type RFC2 3'-UTR plasmid and miR-744-5p mimic showed ~50% reduced luciferase activity compared with cells co-transfected with wild-type RFC2 3'-UTR plasmid and miR-NC. However, no change was observed in cells co-transfected with the mutant RFC2 3'-UTR plasmid (Fig. 4B). This suggested that miR-744-5p directly bound to the 3'-UTR of RFC2. RT-qPCR analysis demonstrated that miR-744-5p expression in GBM tissues was ~50% lower than that in normal-adjacent tissues (Fig. 4C). A significant negative correlation was found between miR-744-5p and RFC2 expression in GBM tissues (Fig. 4D). Additionally, the results revealed that miR-744-5p levels were downregulated by ~50% in U87 cells and 25% in U251 cells compared to NHAs (Fig. 4E). Overall, RFC2 acts as a negative downstream target of miR-744-5p in GBM. U251 and U87 cells were transfected with RFC2-OE and miR-744-5p inhibitor, or si-RFC2 together with miR-744-5p inhibitor. RT-qPCR analysis confirmed that cells transfected with RFC2-OE and miR-744-5p inhibitor showed more than 2.5-fold higher expression of RFC2, and 50% lower expression of RFC2 in cells transfected with si-RFC2 than in the control cells. Cells transfected with si-RFC2 and miR-744-5p inhibitor showed the same level as control cells (Fig. 4F). RFC2 protein expression was markedly increased in cells transfected with miR-744-5p inhibitor, and significantly reduced by in si-RFC2 cells, compared with the controls. Cells transfected with si-RFC2 and miR-744-5p inhibitor showed the same levels of RFC2 expression as the control cells (Fig. 4G).

miR-744-5p targets RFC2 to suppress GBM progression. To assess the important role of miR-744-5p and RFC2 in GBM, NC and si-RFC2, miR-744-5p inhibitor, and Si-RFC2 together with miR-744-5p inhibitor were transfected into U251 and U87 cells. CCK-8 assay analysis showed that after 48 h, cells transfected with miR-744-5p inhibitor exhibited significantly enhanced proliferation capacity, whereas cells transfected with si-RFC2 showed significantly reduced capacity, compared with the control cells. Cells transfected with si-RFC2 and miR-744-5p inhibitor showed the same level as control cells (Fig. 5A). Furthermore, proliferation was enhanced by ~50% in cells transfected with miR-744-5p inhibitor but decreased by ~30% in si-RFC2 cells compared to control cells. Cells transfected with si-RFC2 and miR-744-5p inhibitor showed the same level as control cells (Fig. 5B). In addition, cells transfected with miR-744-5p inhibitor showed ~30% enhanced migratory ability, while cells transfected with si-RFC2 showed ~50% decrease in migratory ability compared to control cells as observed by wound healing assay. Cells transfected with si-RFC2 and miR-744-5p inhibitor showed the same level as control cells (Fig. 5C). Moreover, cells transfected with si-RFC2 exhibited a 40% decrease in cell adhesion, while cells transfected with miR-744-5p inhibitor showed a 40% increase in cell adhesion levels compared to control cells. Cells transfected with si-RFC2 and miR-744-5p inhibitor showed the same level as control cells (Fig. 5D). Additionally, cells transfected with si-RFC2 showed >4-fold caspase-3 activity, while cells transfected with miR-744-5p inhibitor showed ~50% reduced caspase-3 activity compared to control cells. Cells transfected with si-RFC2 and miR-744-5p inhibitor showed the same level as control cells (Fig. 5E). Furthermore, western blotting showed that in U251 and U87 cells, with low expression of miR-744-5p, the expression levels of Bax protein, were lower than those in the control group, while the expression levels of Bcl-2 protein was higher than that in the control group (Fig. 5F). Moreover, the protein expression levels of Bax and Bcl-2 in RFC2 and miR-744-5p knockdown cells were the same as that in the control group (Fig. 5F). Collectively, these results revealed that miR-744-5p suppressed cellular proliferation, migration and adhesion, and promoted apoptosis in GBM by inhibiting RFC2.

Discussion

GBM is the most lethal form of primary glioma (24). The standard therapy for GBM consists of surgery followed by radiation therapy with adjuvant chemotherapy (25,26). The highly infiltrative, heterogeneous and mutable nature of GBM frequently contributes to tumor recurrence and treatment failure (27). Therefore, despite advances in multimodal therapies, the 5-year survival rate of patients with GBM is only 5% after diagnosis (28). Hence, it is necessary to investigate the therapeutic methods for GBM at the molecular level. In the present study, the expression of RFC2 was found to be significantly upregulated in GBM tumor tissues and cell lines, while the expression of miR-744-5p was downregulated. In addition, miR-744-5p targeted RFC2 and functionally repressed its expression, thereby suppressing the progression of GBM cells.

Recently, an increasing number of reports has emphasized the molecular mechanism and significance of miR-744-5p expression in different human tumors. Studies have shown that

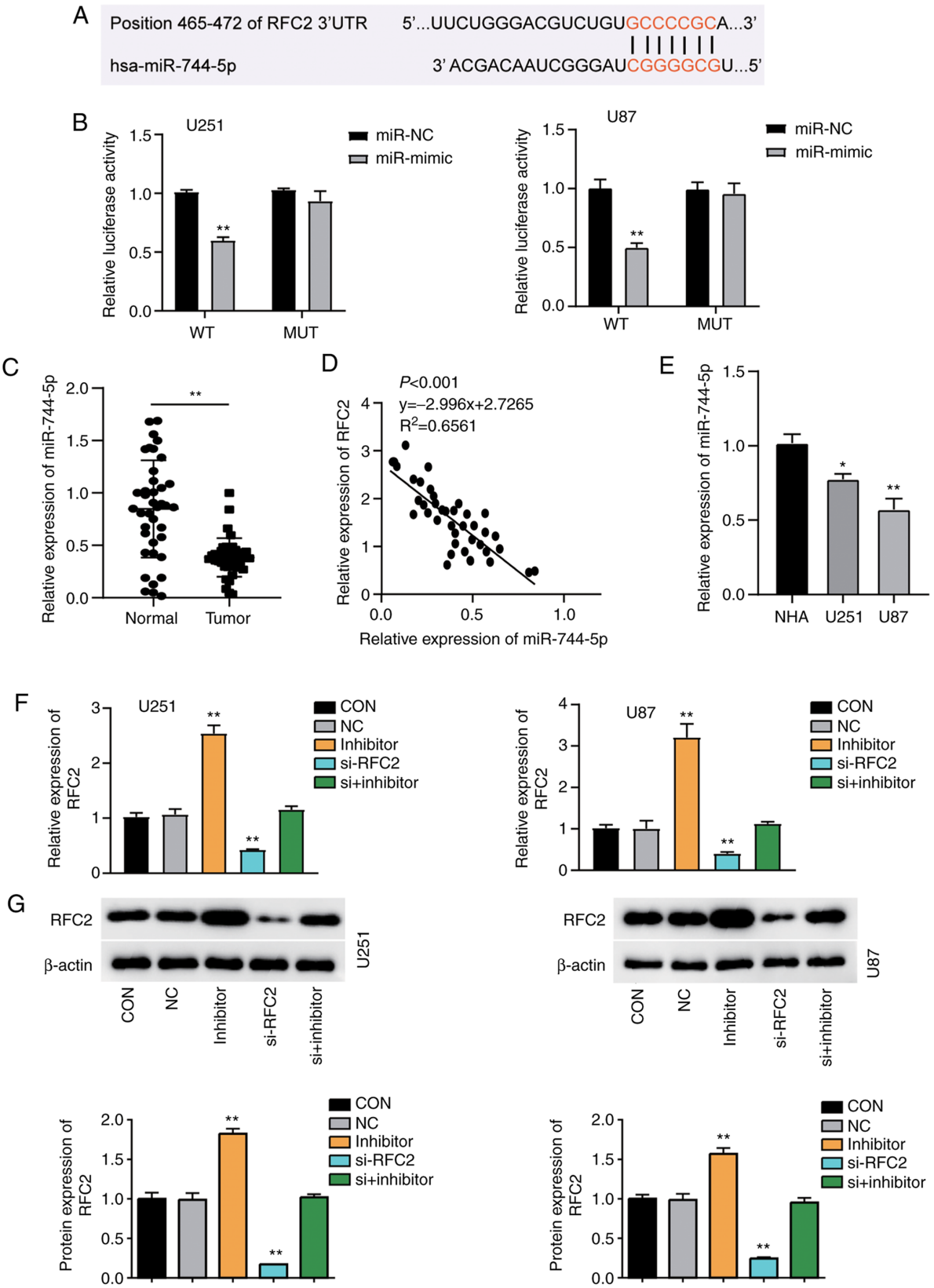

Figure 4. RFC2 is a direct target of miR-744-5p in GBM. (A) Bioinformatics analysis showed the predicted binding sequence of RFC2 3'-UTR. (B) Dual luciferase assay was performed in cells co-transfected with WT RFC2 plasmid or MUT RFC2 plasmid and miR-NC or miR-744-5p mimic in U251 and U87 cells. **P<0.001, one-way ANOVA with Tukey's test. (C) Expression of miR-744-5p in GBM tumor tissues (n=39) and adjacent controls (n=39) from patients with GBM was analyzed by RT-qPCR. **P<0.001, compared with Normal group using paired Student's t-test. (D) Correlation between RFC2 and miR-744-5p expression in GBM tissues. (E) RT-qPCR detection of RFC2 expression in NHA, U251 and U87 cells. *P<0.05 and **P<0.001 compared with NHA using one-way ANOVA with Dunnett's test. (F) RT-qPCR analysis of the mRNA expression of RFC2 in U251 and U87 cells transfected with NC, miR-744-5p inhibitor, si-RFC2, and Si-RFC2+ miR-744-5p inhibitor. (G) Western blot analysis of RFC2 protein expression in U251 and U87 cells transfected with NC, miR-744-5p inhibitor, si-RFC2, and si-RFC2+ miR-744-5p inhibitor. (F-G) CON, blank control; NC, negative control. **P<0.001 compared with CON using one-way ANOVA with Dunnett's test. RFC2, replication factor C subunit 2; GBM, glioblastoma; RT-q, reverse transcription-quantitative; si(RNA), small interfering; OE, overexpression; NC, negative control; WT, wild-type; MUT, mutant; miR, microRNA.

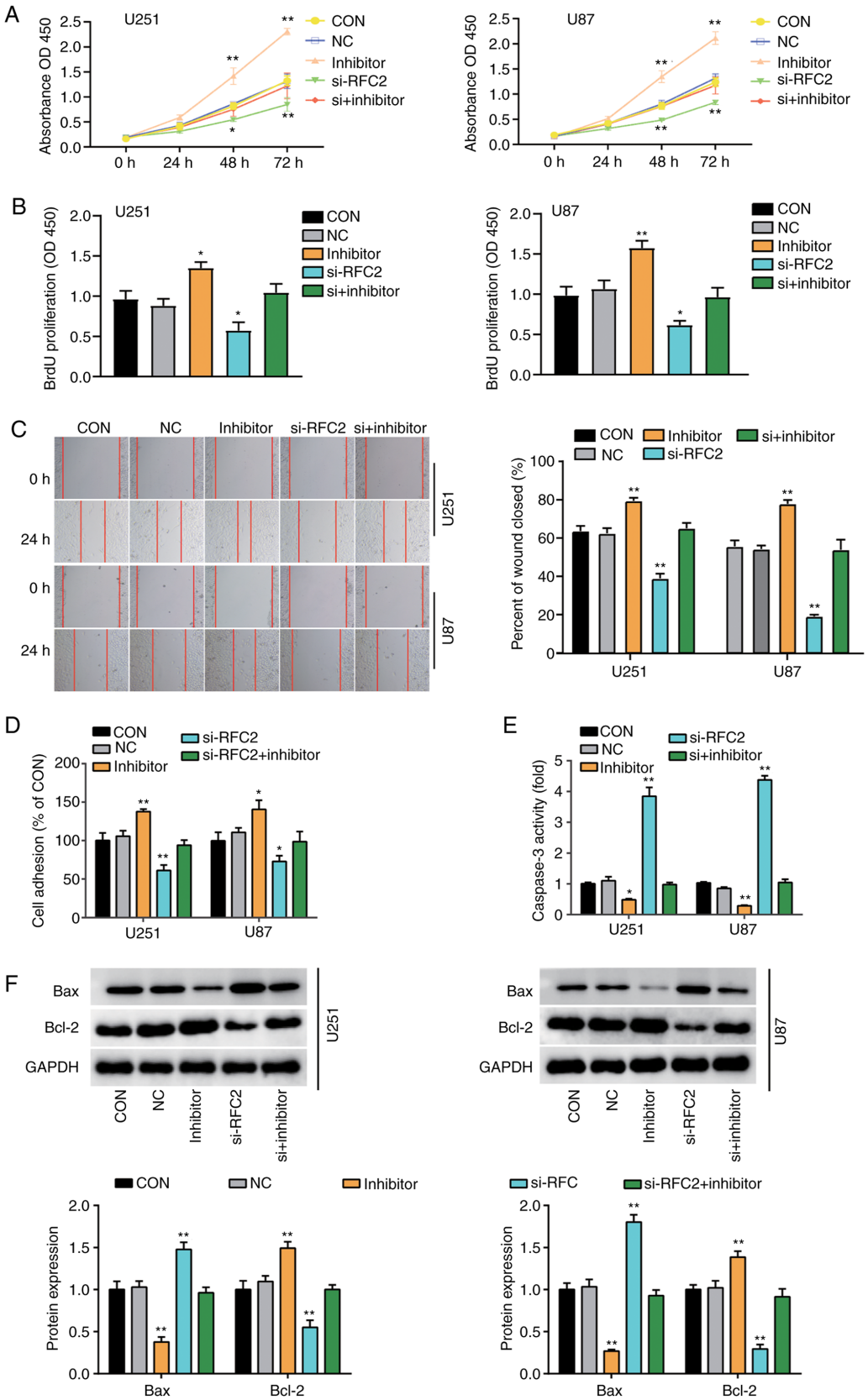

Figure 5. miR-744-5p targeting to RFC2 suppresses glioblastoma progression. (A) Viability of U251 and U87 cells transfected with NC, miR-744-5p inhibitor, Si-RFC2, and Si-RFC2+ miR-744-5p inhibitor was determined by Cell Counting Kit 8 analysis. (B) Proliferation was detected in U251 and U87 cells transfected with NC, miR-744-5p inhibitor, Si-RFC2, and Si-RFC2+ miR-744-5p inhibitor by BrdU assay. (C) Wound-healing assay was performed in U251 and U87 cells transfected with NC, miR-744-5p inhibitor, Si-RFC2, and Si-RFC2+ miR-744-5p inhibitor. (D) Adhesion ability was detected in U251 and U87 cells transfected with NC, miR-744-5p inhibitor, Si-RFC2, and Si-RFC2+ miR-744-5p inhibitor. (E) Caspase-3 activity was determined in U251 and U87 cells transfected with NC, miR-744-5p inhibitor, Si-RFC2, and Si-RFC2+ miR-744-5p inhibitor by caspase-3 activity assay kit. (F) Protein expression levels of Bax and Bcl-2 were determined in U251 and U87 cells transfected with NC, miR-744-5p inhibitor, Si-RFC2, and Si-RFC2+ miR-744-5p inhibitor by western blot assay. *P<0.05 and **P<0.001, compared with CON using one-way ANOVA with Dunnett's test. CON, blank control; NC, negative control; Si-RFC2, SiRNA-RFC2; Si-RFC2+ miR-744-5p inhibitor, SiRNA-RFC2+ miR-744-5p inhibitor; RFC2, replication factor C subunit 2.

abnormal expression of miRNAs may be one of the primary reasons for the occurrence of GBM, and therefore, miRNAs can be used as predictive biomarkers for the diagnosis of GBM (29,30). The expression of miRNA-744-5p in GBM has also been investigated in recent years. For instance, miRNA-744-5p inhibited tumorigenesis by inhibiting NIN1/RPN12 binding protein 1 homolog (NOB1) in GBM (17). The study demonstrated that miRNA-744-5p expression was significantly reduced in GBM tissues and cell lines, and that it inhibited the proliferation, colony formation, migration and invasiveness, and promoted apoptosis in GBM cells by targeting NOB1. Another study revealed that the expression of miR-744-5p was markedly decreased in GBM specimens and primary GBM cell lines. miR-744-5p inhibited GBM migration by suppressing transforming growth factor β1 and Dishevelled 2, which further functionally downregulated MAP2K4 signaling (17). Consistent with their results, the present study indicated that miR-744-5p was significantly decreased in GBM specimens and cell lines. Downregulation of miR-744-5p enhanced proliferation and repressed apoptosis in GBM cells, as observed by CCK-8, wound-healing, and caspase-3 activity assays.

RFC2, a member of the RFC family, acts as a primer recognition factor for DNA polymerase, and regulates cellular proliferation, migration, invasiveness and metastasis in various cancers (18,22). Previous studies have reported the dysregulation of RFC2 in various human cancer types (19,31). For instance, high expression of RFC2 has been considered as a molecular marker of nasopharyngeal carcinoma (19). Ho *et al* (21) observed that miR-4749-5p inhibited RFC2 expression, which further enhanced TMZ cytotoxicity in GBM. They further clarified that a higher level of RFC2 was observed in GBM patients with poor survival. Upregulated miR-4749-5p targeting RFC2 decreased cell viability, increased apoptosis and enhanced TMZ cytotoxicity in GBM cells. In the present study, abnormally increased expression of RFC2 was observed in both GBM tissues and cells. Upregulation of RFC2 enhanced cellular proliferation, migration and adhesion, and suppressed apoptosis in GBM. Furthermore, it was also identified that the impact of RFC2 on GBM cell proliferation, migration, adhesion and apoptosis was regulated by miR-744-5p, which directly targets RFC2.

During the advanced stages of cancer, synaptosomal, associated protein of 25 kDa (SNAP-25), a membrane-binding protein in neurons, is thought to promote tumor development through autophagy, and to play a role in the process of tumor pain (32,33). Furthermore, studies have shown that the expression of SNAP-25 alters the characteristics of synaptic transmission, leading to pathological changes in neuronal circuits in psychiatric diseases (34). Therefore, the effect of miR-744-5p/RFC2 on SNAP-25 is a focus of future research. In addition, the detection of apoptosis-related factors in cancer cells is important when exploring the genesis and development of GBM. For example, E3 ubiquitin-protein ligase XIAP, belonging to the inhibitor of apoptosis protein (IAP) family, is highly expressed in various tumor types, such as malignant glioma (35). p53 mutation may not only lead to the development of GBM tumors (as an early event), but also lead to its malignant progression (as a late event) (36). It has been speculated that XIAP or p53 may be highly expressed in GBM and regulated by the miR-744-5p/RFC2 axis, and this hypothesis will be verified in future studies. Various types of cells exist in the microenvironment of primary, invasive and metastatic tumors (37). The expression levels of miR-744-5p and RFC2 in GBM tissues do not fully reflect the true status of cancer cells. Therefore, the effect of the miR-744-5p/RFC2 axis in GBM requires clinical investigation in greater detail. TMZ resistance is a common cause of treatment failure in GBM (38). A previous study revealed that miR-4749-5p inhibited RFC2 expression, which could further enhance TMZ cytotoxicity in GBM (21). Therefore, we hypothesize that miR-744-5p enhances the chemosensitivity of TMZ in GBM by targeting RFC2, which is also a focus of our future research. Besides, Weighted Gene Co-expression Network Analysis (WGCNA) is a tool often used to identify the key biological processes and hub genes in GBM by constructing gene co-expression networks (39-41), which is different from GEPIA used in the present study. Due to the lack of WGCNA technology, we will learn WGCNA to help us identify the biological processes and genomic networks to develop effective treatment strategies for GBM by targeting the miR-744-5p/RFC2 axis. Moreover, this study only observed these tumor characteristics at the cellular level, detected cell apoptosis by western blot assay and detected cell adhesion by spectrophotometry; however, these findings need to be further determined by establishing animal models, performing flow cytometry and using atomic force microscope.

In conclusion, the results of the present study demonstrated that miR-744-5p targeted RFC2 and suppressed the progression of GBM through repressing cell proliferation and migration, and effectively promoting cell apoptosis. Consequently, our study demonstrated that the miR-744-5p/RFC2 interaction could be a potential candidate for the treatment of GBM.

Acknowledgements

Not applicable.

Funding

The present study was supported by the Fundamental Research Funds for the Central Universities (grant. no. 2019kfyXKJC071).

Availability of data and materials

The datasets used and/or analyzed during the current study are available from the corresponding author on reasonable request.

Authors' contributions

FF and DY performed the experiments and data analysis. PY conceived and designed the study. XJ and JH acquired the data, and are responsible for the authenticity of the raw data. FF and DY conducted the analysis and interpretation of data. All authors read and approved the manuscript.

Ethics approval and consent to participate

The present study was approved by the Ethics Committee of the Union Hospital, Tongji Medical College, Huazhong University of Science and Technology. The processing of clinical tissue samples is in strict compliance with the ethical standards of the Declaration of Helsinki. All patients signed written informed consent.

Patient consent for publication

Not applicable

Competing interests

The authors declare that they have no competing interests.

References

1. Wen PY and Kesari S: Malignant gliomas in adults. New Engl J Med 359: 492-507, 2008.
2. Ostrom QT, Gittleman H, Truitt G, Boscia A, Kruchko C and Barnholtz-Sloan JS: CBTRUS statistical report: Primary brain and other central nervous system tumors diagnosed in the United States in 2011-2015. Neuro Oncol 20 (Suppl 4): iv1-iv86, 2018.
3. Patel NP, Lyon KA and Huang JH: The effect of race on the prognosis of the glioblastoma patient: A brief review. Neurol Res 41: 967-971, 2019.
4. Taphoorn MJ, Sizoo EM and Bottomley A: Review on quality of life issues in patients with primary brain tumors. Oncologist 15: 618-626, 2010.
5. Bartel DP: MicroRNAs: Target recognition and regulatory functions. Cell 136: 215-233, 2009.
6. Pasquinelli AE: MicroRNAs and their targets: Recognition, regulation and an emerging reciprocal relationship. Nat Rev Genet 13: 271-282, 2012.
7. Li XT, Wang HZ, Wu ZW, Yang TQ, Zhao ZH, Chen GL, Xie XS, Li B, Wei YX, Huang YL, *et al*: miR-494-3p regulates cellular proliferation, invasion, migration, and apoptosis by PTEN/AKT signaling in human glioblastoma cells. Cell Mol Neurobiol 35: 679-687, 2015.
8. Chae DK, Park J, Cho M, Ban E, Jang M, Yoo YS, Kim EE, Baik JH and Song EJ: MiR-195 and miR-497 suppress tumorigenesis in lung cancer by inhibiting SMURF2-induced TGF-β receptor I ubiquitination. Mol Oncol 13: 2663-2678, 2019.
9. Shen J and Li M: MicroRNA-744 inhibits cellular proliferation and invasion of colorectal cancer by directly targeting oncogene notch1. Oncol Res 26: 1401-1409, 2018.
10. Chen XF and Liu Y: MicroRNA-744 inhibited cervical cancer growth and progression through apoptosis induction by regulating Bcl-2. Biomed Pharmacother 81: 379-387, 2016.
11. Wang J, Cai H, Dai Z and Wang G: Down-regulation of lncRNA XIST inhibits cell proliferation via regulating miR-744/RING1 axis in non-small cell lung cancer. Clin Sci (Lond) 133: 1567-1579, 2019.
12. Guo Q, Zhang Q, Lu L and Xu Y: Long noncoding RNA RUSC1-AS1 promotes tumorigenesis in cervical cancer by acting as a competing endogenous RNA of microRNA-744 and consequently increasing Bcl-2 expression. Cell Cycle 19: 1222-1235, 2020.
13. Miyamae M, Komatsu S, Ichikawa D, Kawaguchi T, Hirajima S, Okajima W, Ohashi T, Imamura T, Konishi H and Shiozaki A: Plasma microRNA profiles: Identification of miR-744 as a novel diagnostic and prognostic biomarker in pancreatic cancer. Br J Cancer 113: 1467-1476, 2015.
14. Kleemann M, Schneider H, Unger K, Sander P, Schneider EM, Fischer-Posovszky P Handrick R and Otte K: MiR-744-5p inducing cell death by directly targeting HNRNPC and NFIX in ovarian cancer cells. Sci Rep 8: 9020, 2018.
15. Chen S, Shi F, Zhang W, Zhou Y and Huang J: miR-744-5p inhibits non-small cell lung cancer proliferation and invasion by directly targeting PAX2. Technol Cancer Res Treat 18: 1533033819876913, 2019.
16. Hübner M, Hinske CL, Effinger D, Wu T, Thon N, Kreth FW and Kreth S: Intronic miR-744 inhibits glioblastoma migration by functionally antagonizing its host gene MAP2K4. Cancers (Basel) 25: 400, 2018.
17. Deng Y, Li Y, Fang Q, Luo H and Zhu G: microRNA-744 is downregulated in glioblastoma and inhibits the aggressive behaviors by directly targeting NOB1. Am J Cancer Res 8: 2238-2253, 2018.
18. Li Y, Gan S, Ren L, YuanL, Liu J, Wang W, Wang X, Zhang Y, Jiang J, Zhang F and Qi X: Multifaceted regulation and functions of replication factor C family in human cancers. Am J Cancer Res 8: 1343-1355, 2018.
19. Xiong S, Wang Q, Zheng L, Gao F and Li J: Identification of candidate molecular markers of nasopharyngeal carcinoma by tissue microarray and in situ hybridization. Med Oncol 28 (Suppl 1): S341-S348, 2011.
20. Xu J, Wang G, Gong W, Guo S, Li D and Zhan Q: The noncoding function of NELFA mRNA promotes the development of oesophageal squamous cell carcinoma by regulating the Rad17-RFC2-5 complex. Mol Oncol 14: 611-624, 2020.
21. Ho KH, Kuo TC, Lee YT, Chen PH, Shih CM, Cheng CH, Liu AJ, Lee CC and Chen KC: Xanthohumol regulates miR-4749-5p-inhibited RFC2 signaling in enhancing temozolomide cytotoxicity to glioblastoma. Life Sci 254: 117807, 2020.
22. Hu T, Shen H, Li J, Yang P, Gu Q and Fu Z: RFC2, a direct target of miR-744, modulates the cell cycle and promotes the proliferation of CRC cells. J Cell Physiol 235: 8319-8333, 2020.
23. Livak KJ and Schmittgen TD: Analysis of relative gene expression data using real-time quantitative PCR and the 2(-Delta Delta C(T)) method. Methods 25: 402-408, 2001.
24. Kato T, Natsume A, Toda H, Iwamizu H, Sugita T, Hachisu R, Watanabe R, Yuki K, Motomura K, Bankiewicz K and Wakabayashi T: Efficient delivery of liposome-mediated MGMT-siRNA reinforces the cytotoxity of temozolomide in GBM-initiating cells. Gene Ther 17: 1363-1371, 2010.
25. Omuro A and DeAngelis LM: Glioblastoma and other malignant gliomas: A clinical review. Jama 310: 1842-1850, 2013.
26. Gilbert MR, Wang M, Aldape KD, Stupp R, Hegi ME, Jaeckle KA, Armstrong TS, Wefel JS, Won M, Blumenthal DT, *et al*: Dose-dense temozolomide for newly diagnosed glioblastoma: A randomized phase III clinical trial. J Clin Oncol 31: 4085-4091, 2013.
27. Cloughesy TF, Cavenee WK and Mischel PS: Glioblastoma: From molecular pathology to targeted treatment. Ann Rev Pathol 9: 1-25, 2014.
28. Johnson DR and O'Neill BP: Glioblastoma survival in the United States before and during the temozolomide era. J Neurooncol 107: 359-364, 2012.
29. Luo JW, Wang X, Yang Y and Mao Q: Role of micro-RNA (miRNA) in pathogenesis of glioblastoma. Eur Rev Med Pharmacol Sci 19: 1630-1639, 2015.
30. Saadatpour L, Fadaee E, Fadaei S, Mansour RN, Mohammadi M, Mousavi SM, Goodarzi M, Verdi J and Mirzaei H: Glioblastoma: Exosome and microRNA as novel diagnosis biomarkers. Cancer Gene Ther 23: 415-418, 2016.
31. Cui JQ, Shi YF and Zhou HJ: Expression of RFC2 and PCNA in different gestational trophoblastic diseases. Ai Zheng 23: 196-200, 2004 (In Chinese).
32. Olbrich K, Costard L, Möser CV, Syhr KMJ, King-Himmelreich TS, Wolters MC, Schmidtko A, Geisslinger G and Niederberger E: Cleavage of SNAP-25 ameliorates cancer pain in a mouse model of melanoma. Eur J Pain 21: 101-111, 2017.
33. Mu Y, Yan X, Li D, Zhao D, Wang L, Wang X, Gao D, Yang J, Zhang H, Li Y, *et al*: NUPR1 maintains autolysosomal efflux by activating SNAP25 transcription in cancer cells. Autophagy 14: 654-670, 2018.
34. Antonucci F, Corradini I, Morini R, Fossati G, Menna E, Pozzi D, Pacioni S, Verderio C, Bacci A and Matteoli M: Reduced SNAP-25 alters short-term plasticity at developing glutamatergic synapses. EMBO Rep 14: 645-651, 2013.
35. Fulda S, Wick W, Weller M and Debatin KM: Smac agonists sensitize for Apo2L/TRAIL- or anticancer drug-induced apoptosis and induce regression of malignant glioma in vivo. Nat Med 8: 808-815, 2002.
36. Shiraishi S, Tada K, Nakamura H, Makino K, Kochi M, Saya H, Kuratsu Ji and Ushio Y: Influence of p53 mutations on prognosis of patients with glioblastoma. Cancer 95: 249-257, 2002.
37. Wu T and Dai Y: Tumor microenvironment and therapeutic response. Cancer Lett 387: 61-68, 2017.
38. She X, Yu Z, Cui Y, Lei Q, Wang Z, Xu G, Xiang J, Wu M and Li G: miR-128 and miR-149 enhance the chemosensitivity of temozolomide by Rap1B-mediated cytoskeletal remodeling in glioblastoma. Oncol Rep 32: 957-964, 2014.
39. Xu P, Yang J, Liu J, Yang X, Liao J, Yuan F, Xu Y, Liu B and Chen Q: Identification of glioblastoma gene prognosis modules based on weighted gene co-expression network analysis. BMC Med Genomics 11: 96, 2018.
40. Xiang Y, Zhang CQ and Huang K: Predicting glioblastoma prognosis networks using weighted gene co-expression network analysis on TCGA data. BMC Bioinformatics 13 (Suppl 2): S12, 2012.
41. Kong Y, Feng ZC, Zhang YL, Liu XF, Ma Y, Zhao ZM, Huang B, Chen AJ, Zhang D, Thorsen F, *et al*: Identification of immune-related genes contributing to the development of glioblastoma using weighted gene co-expression network analysis. Front Immunol 11: 1281, 2020.